Hydrological Sciences Journal

ISSN: 0262-6667 (Print) 2150-3435 (Online) Journal homepage: http://www.tandfonline.com/loi/thsj20

Structural uncertainty assessment in a discharge simulation model

Xiaoyong Zhang , Georg Hörmann , Junfeng Gao & Nicola Fohrer

To cite this article: Xiaoyong Zhang , Georg Hörmann , Junfeng Gao & Nicola Fohrer (2011) Structural uncertainty assessment in a discharge simulation model, Hydrological Sciences Journal, 56:5, 854-869, DOI: 10.1080/02626667.2011.587426

To link to this article: https://doi.org/10.1080/02626667.2011.587426

Published online: 12 Jul 2011.

Structural uncertainty assessment in a discharge simulation model

Xiaoyong Zhang[1], Georg Hörmann[1], Junfeng Gao[2] & Nicola Fohrer[1]

[1]*Ecology Centre, Department of Hydrology and Water Resources Management, University of Kiel, Olshausenstrasse 75, D-24118 Kiel, Germany*
xzhang@ecology.uni-kiel.de

[2]*Nanjing Institute of Geography & Limnology, Chinese Academy of Sciences, Nanjing 210008, China*

Received 21 February 2008; accepted 10 February 2011; open for discussion until 1 January 2012

Citation Zhang, X. Y., Hörmann, G., Gao, J. F. & Fohrer, N. (2011) Structural uncertainty assessment in a discharge simulation model. *Hydrol. Sci. J*. **56**(5), 854–869.

Abstract A major goal in hydrological modelling is to identify and quantify different sources of uncertainty in the modelling process. This paper analyses the structural uncertainty in a streamflow modelling system by investigating a set of models with increasing model structure complexity. The models are applied to two basins: Kielstau in Germany and XitaoXi in China. The results show that the model structure is an important factor affecting model performance. For the Kielstau basin, influences from drainage and wetland are critical for the local runoff generation, while for the XitaoXi basin accurate distributions of precipitation and evapotranspiration are two of the determining factors for the success of the river flow simulations. The derived model uncertainty bounds exhibit appropriate coverage of observations. Both case studies indicate that simulation uncertainty for the low-flow period contributes more to the overall uncertainty than that for the peak-flow period, although the main hydrological features in these two basins differ greatly.

Key words hydrological modelling; perceptual model; model structural uncertainty; Kielstau, Germany; XitaoXi, China; PCRaster

Evaluation de l'incertitude structurelle d'un modèle de simulation de débit

Résumé Un objectif majeur de la modélisation hydrologique est d'identifier et de quantifier les différentes sources d'incertitude au fil du processus de modélisation. Cet article analyse l'incertitude structurelle d'un système de modélisation du débit en considérant un ensemble de modèles de complexité structurelle croissante. Les modèles sont appliqués à deux bassins: Kielstau en Allemagne et XitaoXi en Chine. Les résultats montrent que la structure du modèle est un facteur important qui affecte la performance du modèle. Pour le bassin de Kielstau, les influences du drainage et des zones humides sont critiques pour la genèse locale de l'écoulement, tandis que pour le bassin de XitaoXi la précision des distributions des précipitations et de l'évapotranspiration est déterminante pour le succès des simulations de débit. Les limites d'incertitude du modèle mettent en évidence une couverture appropriée des observations. Les deux études de cas indiquent que l'incertitude de simulation en période d'étiage contribue davantage à l'incertitude globale que celle des périodes de crue, bien que les principales caractéristiques hydrologiques de ces deux bassins soient très différentes.

Mots clefs modélisation hydrologique; modèle perceptuel; incertitude structurelle de modélisation; Kielstau, Allemagne; XitaoXi, Chine; PCRaster

1 INTRODUCTION

Hydrological models are always simplifications of the reality, and are therefore all subject to varying degrees of uncertainty. It is commonly accepted that the model uncertainty stems from a variety of sources where it can affect the model predictions (Melching 1995, Gupta *et al*. 2005). For example, many data sets needed as model inputs are defined through measurement in the field or laboratory, which introduces measurement errors and generates "data-driven uncertainty" (Brown and Heuvelink 2005). Then the estimation of parameters and formalization of model structure may lead to "explanatory uncertainty" (Brown and Heuvelink 2005) in model predictions. Some model parameters are inherently uncertain when they refer to real, measurable quantities such as soil hydrological conductivity, while some are

ISSN 0262-6667 print/ISSN 2150-3435 online

doi: 10.1080/02626667.2011.587426
http://www.informaworld.com

empirical quantities applied to models and must therefore be estimated using measurements of the system inputs and outputs. Rather, we are uncertain about the errors in our understanding of the real system represented in the model structure. The natural flow systems that are themselves imperfectly known and understood have to be translated in the hydrological models. This is particularly important because models are more frequently used but observations are still limited.

In recent years, uncertainty of hydrological models has been investigated extensively, in particular the uncertainty induced by model inputs and parameter values (e.g. Rogers *et al*. 1985, Clausnitzer *et al*. 1998, Haan *et al*. 1998, Hansen *et al*. 1999, Beven and Freer 2001, Christiaens and Feyen 2002, Carpenter and Georgakakos 2004, Vrugt *et al*. 2005, 2006, Gourley and Vieux 2006, Lindenschmidt 2006, Ratto *et al*. 2007, Choi and Beven 2007). This abundance of literature does not imply that the modelling uncertainty from the change of model structure can be neglected (Beven *et al*. 2007). Indeed, uncertainty induced by model structures can be more significant than parameter and input data uncertainty, but such uncertainties are difficult to assess explicitly or to separate from other uncertainties during the calibration process (Beven and Binley 1992, Lindenschmidt *et al*. 2007). Furthermore, according to Beven (2001), model structures can only be identified uniquely when two components are specified: the perceptual model describing the dominant flow processes, and the conceptual model that is the mathematical definition of those processes. Considered as one type of "explanatory uncertainty", structural uncertainty is defined as the modelling uncertainty due to the selection of an appropriate model, which includes the defined hydrological processes (perceptual model) and the mathematical description of these processes (conceptual model). In this context, the perceptual model might be more uncertain in comparison with the conceptual part, since it is usually formed based on a perceived lack of knowledge about the real processes, or a belief that the model abstracts and simplifies known processes (Neuman 2002, Beven 2001). For example, Newton's laws only resolve transfers of energy, matter and momentum through the environment. They do not resolve the processes that lead to changes in the storage and transfer of these elementary units. In practice, we are usually interested in the processes, as well as the transfers, because dominant process controls change through time and space.

Whereas the structural uncertainty is of more interest and importance, the range of schemes available for assessing the impact of model structure on modelling uncertainty is quite limited. Many investigations in model structures are mixed with other sensitivity or uncertainty analysis, such as parameter estimation, different discretizations or runtime errors (e.g. Uhlenbrook *et al*. 1999, Butts *et al*. 2004, Ewen *et al*. 2006, Lindenschmidt *et al*. 2007, Son and Sivapalan 2007). Some studies (e.g. Schuol and Abbaspour 2006) have discussed the impact of model structure and model complexity on model performance, but did not address the issues of structural uncertainty separately. Butts *et al*. (2004) explored ten model structures with different definitions in flow processes, built-in equations and spatial distributions; root mean square error (RMSE) and correlation (R) were used to assess the performance of model structure ensembles. Lindenschmidt *et al*. (2007) placed emphasis on the uncertainty in equations, and the quantification of structural uncertainty is quite case-specific as it is applied in a water quality modelling system. Yang *et al*. (2007) did not separate input and model structural uncertainty and concluded that a high fraction of uncertainty is due to input and model structure, comparing to parameter uncertainty.

In this study, we changed the model structure (mainly in perceptual models) to facilitate the structural uncertainty analysis. Different model structures were set up with PCRaster (Van Deursen 1995, Wesseling *et al*. 1996), a spatial modelling language and system. We explored the impact of different model structures on the discharge simulations for two catchments: Kielstau—a small lowland catchment in northern Germany, and XitaoXi—a mesoscale mountainous basin in the south of China. With given model inputs, we focus on the uncertainty assessment in model structure. The results of the model ensembles are assessed against a number of performance criteria for the river discharge. The derived uncertainty bounds are quantified and more detailed structural uncertainty analysis is performed using peak-flow/low-flow split testing.

With the development of a hydrological modelling framework that permits changes in the model structure and increases the model complexity within the same modelling tool, the objectives of this paper are: (a) to evaluate the performance of different model structures; (b) to identify the important hydrological processes or factors affecting model performance for each catchment; and (c) to estimate the structural uncertainty associated with river discharge simulation.

2 THE STUDY SITES AND DATA PREPARATION

We report in this paper the estimates of daily streamflow of two representative basins differing in all main geohydrological features (Zhang *et al*. 2009). It is thought that the selection of two different basins would be useful in optimal exploitation of their perceptual model structures and of the flexibility of the employed modelling tool. This work is also one part of a Sino-German integrated geohydrological study of two basins, comprising hydrological and geophysical surveys, the collection of hydrometeorological and hydrochemical data, streamflow simulation, exploratory water quality investigation, model uncertainty, etc. It aimed to facilitate a systematic exploitation of the river water resources.

Figure 1 shows the approximate geographical locations and the digital elevation map of the two basins that were selected for the integrated geohydrological studies, namely the Kielstau basin and the XitaoXi basin.

2.1 The Kielstau basin

The Kielstau basin is located in Schleswig-Holstein, northern Germany, and covers an area of 51.5 km^2. The River Kielstau, approx. 11 km long, is a small stream draining the basin from northeast to southwest. The landscape is distinguished by a rather flat relief, owing to the landform process under the influence of extensive glaciation during the Pleistocene epoch. The glaciers moved back and forth in turn over long periods of time creating on this small area a mixture of different types of moraine in close succession. The whole watershed has poor drainage due to the low gradient with a maximum altitude difference of 55 m (see Fig. 1, left). Wedged between the North Sea and the Baltic Sea, the Kielstau catchment is characterized by moderate temperature and oceanic climate with mild, moist winters and cool, rainy summers. Snowfall is rare and occurs, on average, on 20 up to 25 days per winter. Average annual precipitation is around 860 mm, and actual evaporation around 400 mm (Schmidtke 1999). The geological basement of the basin is dominated by Pleistocene deposits, resulting in a wide variety of soil types and soil forms in this small area. Soils mainly consist of podzol, gleysol and luvisol, formed in the Saale and Weichsel ice ages, among which gleysol belongs to the major wetland soil types (Sponagel 2005). These are heavy soils having high field capacity and containing large proportions of clay and silt, which contribute to the formation of numerous scattered "Niedermoor" and "Hochmoor" (peatland or wetland) in the watershed.

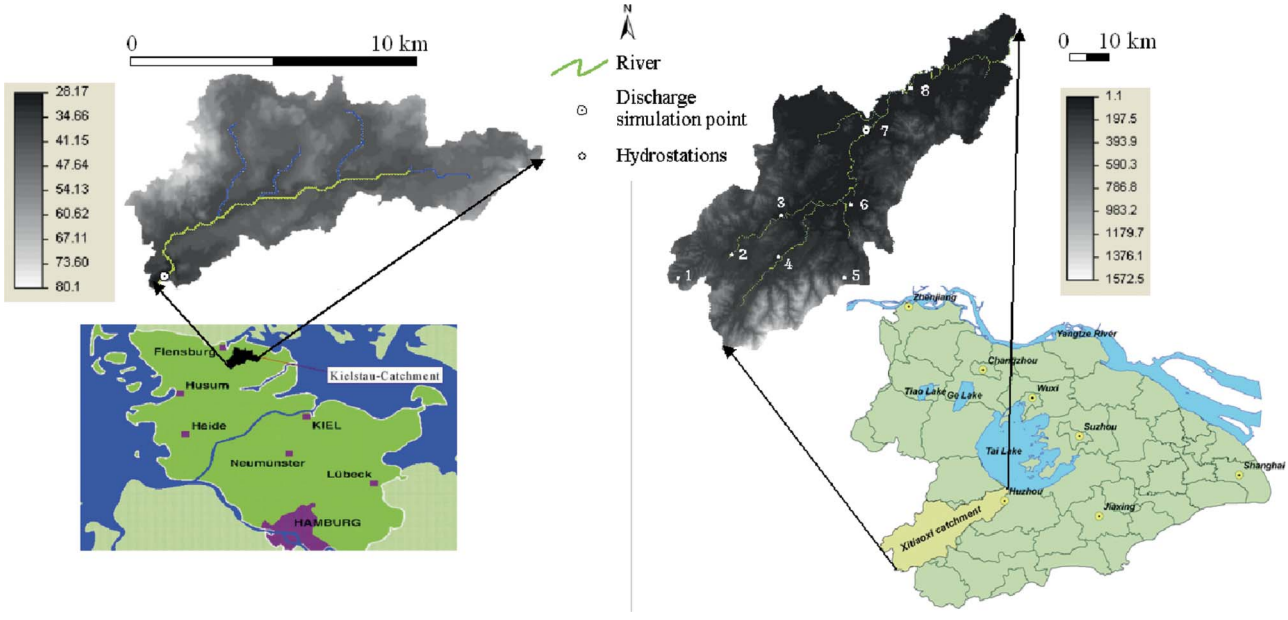

Fig. 1 Location and DEM map of the two study catchments (Zhang *et al*. 2009): discharge simulation point for Kielstau: Soltfelt; and for XitaoXi: Hengtangcun, hydrostation. 1: Tianjintang, 2: Hanggai, 3: Fushishuiku, 4: Laoshikan, 5: Yinkeng, 6: Dipu, 7: Hengtangcun, 8: Fanjiacun.

A large fraction of wetland area and near-surface groundwater level are observed in this region (Trepel 2004), but there are no accurate mapping data for this. The dynamics of near-surface groundwater are generally determined by precipitation, and, when close to the river, by stream water level as well. In most cases, groundwater levels in the riparian wetland are higher than those in the river. The interaction between surface water and groundwater is thus active for this region, especially in the riparian wetland area. During flood events, a reversal of the flow direction could occur if the close-to-river groundwater level is lower than the stream water level (Springer 2006).

2.2 The XitaoXi basin

The second study area, XitaoXi, is a 2271 km^2-sized mountainous basin located in southeast China. It is one of the major sub-basins of Taihu Lake. From the elevation map in Fig. 1 (right), it may be seen that the topographic slope declines from southwest to northeast. In general, the whole XitaoXi basin can be characterized by three different areas with distinct topography: the upper reaches in the southeastern part are mountainous, with elevation over 600 m, accounting for about 15% of the total basin area; a 150–600-m-high hilly area in the centre accounts for 40%; and in the remaining northeastern part the topography turns into a flat outwash plain with a low hydraulic gradient. The dominant soil types are red soil and rocky soil. The ecologically and geologically diverse XitaoXi area is characterized by changing land-use patterns. The mountainous upper reaches are dominated by forest, of which about 75% has been planted with bamboo; in the middle hilly reaches, farmland and forest are in nearly equal percentage, while the downstream plain areas are mainly paddy fields (Wan *et al*. 2007). As it is situated in a semi-tropical climate zone, rainfall in the basin is monsoonal. The spatio-temporal variations in precipitation and evaporation distribution are statistically significant (Gao *et al*. 2006). Rainfall usually commences in the middle of May and continues mainly during June, July, August and September. Occasional showers occur in other months. There is usually more rainfall in the mountains than in the neighbouring plains. The average annual rainfall recorded at the eight hydrometeorological stations (Fig. 1, right) in XitaoXi basin for the years 1979–1988 was found to be 1466 mm. The annual rainfall gradually decreased from the southwest mountain area (1800 mm) to the northeast plains (1200 mm). Annual open pan evaporation for this period was estimated as 800–900 mm. Evaporation intensity from the southwest to the northeast has shown an increasing trend (Zhang *et al*. 2006). The drainage pattern in the XitaoXi basin is of dendritic type. Two reservoirs—Fushishuiku and Laoshikan (near hydrostations 3 and 4 in Fig. 1)—in the upstream areas are used for flood control in rainy seasons. The only available continuous streamflow data are recorded at the Hengtangcun and Fanjiacun stations. The river runoff values at Fanjiacun were greatly influenced by the backflow from Taihu Lake, owing to its location in the lower outwash plain, close to the XitaoXi basin outlet to Taihu Lake. In order to facilitate the comparison of runoff simulations with the measured values, the Hengtangcun station, which covers the discharge basin area of 1524 km^2, was chosen in this study as the simulation point.

2.3 Data

The data used in the PCRaster model are: climatic data, DEM, soil and land-use data. The climatic data for Kielstau catchment were taken from the data set of Flenburg station, 9 km north of Kielstau basin (German Weather Service, Deutscher Wetterdienst, DWD). The DEM was provided by Landesvermessungsamt Kiel, and the LANU (Landesamt für Natur und Umwelt) provided river discharge values from 1983 to 1999 (at the official Soltfeld gauge station). Other spatial data such as land use and soil maps are from the BGR (Bundesamt für Geowissenschaften und Rohstoffe). Land use in the Kielstau basin is predominantly agricultural (55.82%) and grass (26.14%). All maps were converted to a raster map with a cell length of 50 m.

Daily precipitation data in the XitaoXi basin are available from eight stations within the watershed area, while evaporation data are only recorded at two stations—Fushishuiku and Hengtangcun. The discharge data set from the selected Hengtangcun gauge station is available from 1978 to 1987. All data including land-use and soil maps were provided by the Administrative Bureau of TaiHu Basin. The cell length of the raster maps is 200 m.

A long-term hydrometeorological analysis was conducted for both basins. The values for annual precipitation, potential ET and river runoff of the two basins are presented in Fig. 2, and Fig. 3 shows the monthly mean values of rain and discharge which can be used to derive seasonal patterns for the two areas (Zhang *et al*. 2008). With the maritime climate environment in the Kielstau region, there is

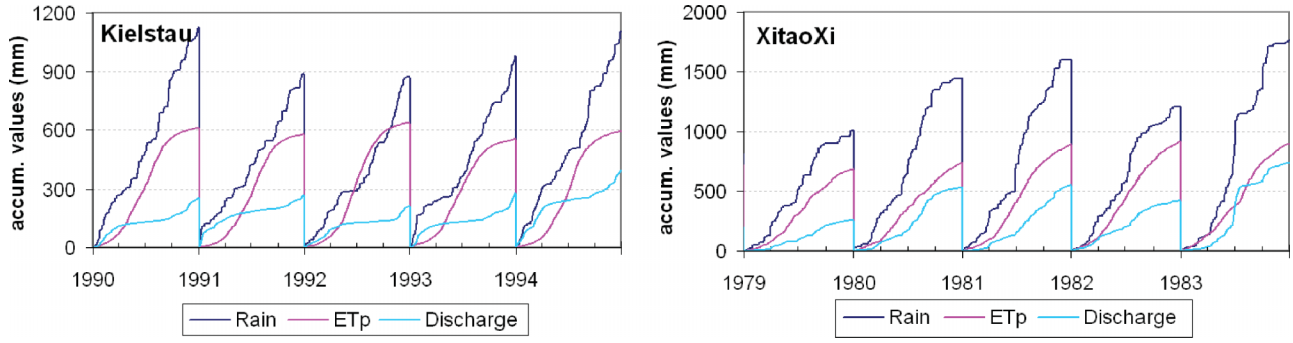

Fig. 2 Annually accumulated climatic data for the Kielstau and XitaoXi catchments.

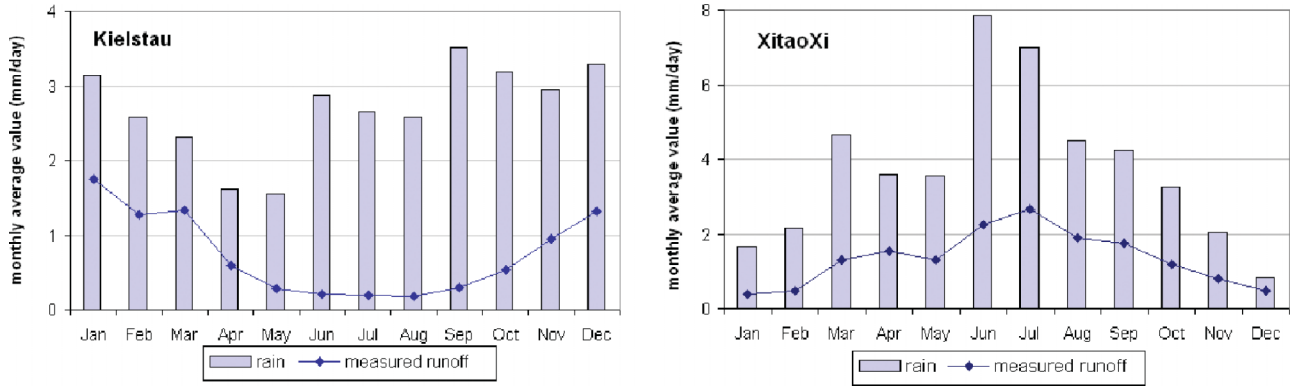

Fig. 3 Monthly rain and discharge mean value, based on data from 1990 to 1999 (for Kielstau), and from 1979 to 1988 (for XitaoXi) (Zhang *et al*. 2008).

precipitation all the year round. Neither the annual variations in rainfall, nor the seasonal ones, extend to severe extremes. Meanwhile, a quite high evapotranspiration rate is shown during the summer season. The seasonal changes of rainfall and runoff are more distinct in the XitaoXi basin because of the monsoon climate, with 75% of rain falling between April and October. The average daily runoff of the XitaoXi River (35.09 m^3/s) is much higher than that of the Kielstau stream (0.45 m^3/s). The difference is also significant when considering the different discharge areas of the selected gauge stations for both basins. The runoff rate per unit area is 8.82 L s^{-1} km^{-2} for Kielstau, and 23.02 L s^{-1} km^{-2} for XitaoXi. Figure 3 also presents different patterns of the two watersheds in streamflow response to summer rains. To have a better look at their correlation, we calculated the runoff efficiency based on the ratio of monthly streamflow to monthly precipitation (Wu and Johnston 2008). The distribution of river runoff in the XitaoXi catchment is mainly controlled by rainfall. The runoff values kept in good correlation with the variation of rainfall, with runoff efficiencies ranging from 0.22 to 0.58. The runoff efficiencies calculated for the Kielstau basin have similar values for winter, with extremely low values for the summer months, e.g. 0.08 for the month of June, making the average value drop to 0.3. The larger variations in runoff efficiency of the Kielstau basin might be caused by high evapotranspiration in the wetland area of the watershed, and its capacity to impound surface runoff or to deter the streamflow events.

3 THE UNCERTAINTY ANALYSIS PROCEDURE

3.1 Basic module description

The basic hydrology module—KIDS (Kielstau Discharge Simulation model)—was developed for practical purposes to facilitate further research in nutrient leaching assessment, water protection and land-use evaluation in the Kielstau area. This implies that relatively simple model approaches were chosen to operate under restricted data availability. The model calculation is based upon the water balance equation (see equation (1)), taking into account interception, precipitation, evapotranspiration (ET), and the flows to other compartments. We use mm as the unit of measure for all the water amount expressions included herein, and calculate with a daily time step:

$$S_t = S_{t-1} + P_t - ET_t - I_t - Q_{ot} - S_{pt} \quad (1)$$

where S is the soil water content, t is the modelling time step (d), P is precipitation, ET is evapotranspiration, I is interception, Q_o is surface runoff (overland flow), and S_p is percolation or seepage.

Precipitation and potential evapotranspiration are required as input data. The model calculates interception from canopy and litter, combined transpiration and evaporation and the water fluxes in the soil column. The calculation of gravity-driven water percolation in the KIDS model follows the semi-empirical differential equation of Glugla (1969). Surface runoff Q_o is calculated according to equation (2). It describes soil percolation and storage calculation on the basis of derived soil parameters such as field capacity and infiltration rate of soil water deficit:

$$Q_o = \max\{[P - I - K_c\,(S_{fk} - S)], 0\} \quad (2)$$

where K_c is the infiltration parameter and S_{fk} is the wetness at field capacity.

The subsurface runoff or lateral flow for the soil column can be subdivided into several layers according to the soil database. This is simplified as one lumped uniform soil column for the basic KIDS model. We adjusted the amount of subsurface runoff with a lateral flow rate parameter as follows:

$$Q_s = K_s S \quad (3)$$

where Q_s is subsurface flow, and K_s is lateral flow rate.

Runoff is then composed of three parts: surface runoff, lateral flow and groundwater discharge from the groundwater layer, which is represented as a linear storage. In the basic model M for both basins, the value of parameter K_s is set equal to zero, whereas in the sub-module L, it is adjusted above zero for better comparison. More details of subsurface flow and groundwater calculation will be explained in Section 3.3.

Flow direction is then determined based on a DEM, and channel flow is modelled with fully dynamic runoff routing using kinematic wave function. The KIDS model represents a rather simple rainfall–runoff model. A very attractive feature is its applicability to small or large-scale areas, and flexibility to adapt model structures, whenever it is appropriate or necessary to take the internal variability of soil and vegetation characteristics, in particular of specific influence factors, into account. This could be done by means of additional sub-modules applied to the basic KIDS structure. Essential references are given in Hörmann *et al*. 2007 and Zhang *et al*. 2007.

3.2 Data processing

Owing to the different sizes of the two basins and the availability of data, it is important to handle data differently to fit in a more appropriate and regionalized model.

The basic module is implemented in the Kielstau basin with a single station for precipitation and ET. The only source of climatic data is from the neighbouring Flensburg weather station, since long-term weather records within the Kielstau area were missing. One short-term data set obtained from field observations was compared with the long-term data set. The temporal variation of rainfall data was identical to the long-term records, except for some marginal differences in daily values. The spatial variation of rainfall may be considered homogeneously distributed around the local area on account of its flat topographical nature. The induced uncertainty is thus expected to be small resulting from the use of alternative climatic input data. As the soil water dynamics is described with the capacity based Glugla approach, the capacity parameters required by the model are attached to the model by external data files that are consistent with the German soil texture classification and their related capacity parameters in AG Boden 2005 (Sponagel 2005).

Meanwhile, deriving quantitative weather information is a more difficult task in mountainous regions such as the XitaoXi basin. Spatially-distributed rainfall or snow is important in a large and mountainous catchment for accurate hydrological prediction. Considering the XitaoXi climatic zone, only rainfall is the significant source in the hydrological cycle. Rainfall data from the eight weather stations within the study area were interpolated using Thiessen polygons. The network of ET gauges is less dense with only two stations in the area. Potential ET values were measured using the Chinese pan method (Gao *et al*. 2006).

3.3 Development of the model structure ensembles

We used the following procedure to create the model ensemble, as shown in Fig. 4. First, a basic module (abbreviated as M) and a group of sub-modules (represented by A, B, C etc.) are required as elementary components to build up a module pool. Secondly, the

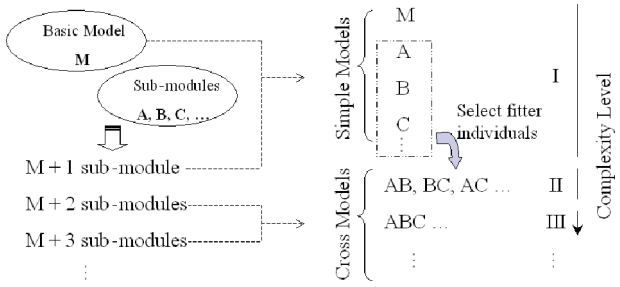

Fig. 4 Schematic chart of the framework to develop model structure ensembles.

basic module M is combined with the other modules to create a group of "simple" models. These simple models are given the same letter as the sub-module. The methodology of "genetic algorithm" was applied to select fitter individuals for the optimization of the model structure combinations. Taking the performance of the basic module M as a reference, only the simple models with improvement in simulation results (according to the selected criteria) are included in the next step. Finally, the basic module M is combined with all other modules to form a series of "cross-models". They are identified with the ID combination of their sub-modules; thus, the main water flow processes of a model ensemble can be easily recognized from its name, and the number of the characters is an indicator of the complexity.

We implemented a suite of model versions, representing the structural uncertainty of both watersheds. The basic KIDS model concept is taken as module M, and six sub-modules are developed for both Kielstau basin (H, L, T, G, D, W) and XitaoXi basin (P, E, G, L, T, R).

3.3.1 Models H and M: Kielstau To describe the potential evapotranspiration (ET_p) two different approaches were used: calculation of ET_p with the empirical Haude formula (Haude 1958) in model H using crop-specific monthly coefficients, and calculation of a reference ET for grass with the FAO Penman-Monteith method (Allen *et al*. 1998) in the basic model M.

Traditionally the Haude evapotranspiration formula (equation (4)) was widely used in Germany with temperature (t in °C) and relative humidity (rH in %) measured at 14:00 h required as inputs. For different types of land use, monthly coefficients (a) for the Haude formula are given reflecting the state of the plants in an average annual growth cycle. Thus:

$$ET_p = ae_{s14}(1 - rH_{14}/100) \quad (4)$$

where a (-) is the Haude coefficient (from monthly tables, crop specific); e_{s14} (hPa) is saturated vapour pressure at 14:00 h local time, calculated based on temperature; and rH_{14} (%) is relative humidity at 14:00 h local time.

The FAO Penman-Monteith formula to estimate the reference evapotranspiration (ET_0) was derived by utilizing some assumed constant parameters and simplifying the air density term, as shown in equation (5). The equation requires standard climatological records of solar radiation (sunshine), air temperature, humidity, and wind speed:

$$ET_0 = \frac{0.408\Delta(R_n - G) + \gamma \frac{900}{T+273} u_2(e_s - e_a)}{\Delta + \gamma(1 + 0.34u_2)} \quad (5)$$

where ET_0 (mm d^{-1}) is reference evapotranspiration, R_n (MJ m^{-2} d^{-1}) is net radiation at the crop surface, G (MJ m^{-2} d^{-1}) is soil heat flux density, T (°C) is mean daily air temperature at 2 m height, u_2 (m s^{-1}) is wind speed at 2 m height, e_s (kPa) is saturated vapour pressure, e_a (kPa) is actual vapour pressure, $e_s - e_a$ (kPa) is the saturated vapour pressure deficit, Δ (kPa $°C^{-1}$) is the slope vapour pressure curve, and γ (kPa $°C^{-1}$) is a psychrometric constant.

The evapotranspiration estimate by the Haude approach was distinctly less satisfactory. The potential ET_p for Haude is only 51 mm $year^{-1}$ higher than the ET_a calculated by the M model. A further analysis of the monthly values shows that the summer evaporation is greatly underestimated and the growth of the plants starts earlier than predicted by the Haude method. The FAO Penman-Monteith method is thus recommended as the standard method for the definition and computation of the reference evapotranspiration to all other models of the Kielstau watershed.

3.3.2 Models G, L and T: Kielstau and XitaoXi A threshold of groundwater outflow to river is set in model G, in order to restrict the impact of groundwater on discharge, as defined by:

$$G_t = G_{t-1} + I_{gt} - Q_{gt} \quad (6)$$

$$Q_g = \min(K_g G, G_m) \quad (7)$$

where G is groundwater storage, I_g the inflow to groundwater aquifer, Q_g the groundwater discharge to runoff, K_g the groundwater outflow rate, and G_m the maximum daily groundwater outflow or groundwater

outflow threshold. Combining equations (6) and (7) yields the daily groundwater dynamics.

The lateral flow model L is adjusted with a positive value of the lateral flow rate K_s, as shown in equation (3). The evapotranspiration for different land-use types or crop surface is considered in model T. For Kielstau, we calculate the crop specific evapotranspiration ET_c for other crops (equation (8)) referring to Penman-Monteith method, with land-use coefficients (K_c) that relate ET_c to ET_0, the standard reference evapotranspiration.

$$ET_c = K_c ET_0 \tag{8}$$

For XitaoXi, the potential evapotranspiration measured by pan method proved its practical value in Jin and Gao (2006). It has been used successfully to estimate reference evapotranspiration by observing the evaporation loss from a water surface and applying empirical coefficients to relate reference evapotranspiration to pan evaporation:

$$ET_r = K_p E_{pan} \tag{9}$$

where ET_r is the reference evapotranspiration in the XitaoXi area, K_p the pan coefficient, and E_{pan} the pan evaporation.

3.3.3 Models D and W: Kielstau In Kielstau large areas of drainage were observed to combat the problem of water logging associated with flat topography and high water tables. The leakage of water from the network of water distribution through the manmade drainage channels is thus another important factor considered in model D, functioning as in equation (10). In this conceptual relationship, the soil types are the function controlling the curvature of drainage volume:

$$D = K_d S + L_d \tag{10}$$

where D is the drained water volume, K_d is a drainage factor, S is the available soil water storage, and L_d is the lateral inflow volume (lateral seepage from irrigation canals and drainage channels).

We introduced an additional wetland layer in model W. The dynamics of wetland water can be described as:

$$W_t = W_{t\text{-}1} + I_{wt} - E_{wt} - Q_{wt} \tag{11}$$

where W is wetland water storage; I_w the incoming water volume influenced by precipitation, interception and soil moisture; E_w the water loss from wetland, mainly evapotranspiration; and Q_w the wetland water seepage contributing to runoff.

Evaporation is frequently the most significant loss of water from a wetland as noted by Tagaki *et al*. (1998). This is also supported by a summery of studies on hydrological functions of wetlands (Bullock and Acreman 2003). Among all the collated reference studies, there is strong evidence that wetlands evaporate more water than other land types, such as grassland, forests or arable land. From the data analysis for Kielstau, the river runoff reveals a similar feature influenced by higher evaporation from wetlands. However, investigations into the wetland evaporation rate for Kielstau suffer from a lack of reliable measurements, as climatic data are not collected routinely from wetland areas. In a review of evapotranspiration rates measured in a Danish wetland study, it was found that wetland evaporation is 1.3 to 1.5 times higher than grassland evaporation (Andersen 2003). Thus, within the framework provided by a water budget investigation, we set a factor of 1.3 times the reference evaporation for the wetland area, to model realistic wetland conditions in the KIDS model. The fraction of wetland is unknown. By reclassifying soil types Peat and Gley soil as wetland, it is estimated as 12%. Another consequential effect of water stagnation is substantial water storage within wetlands. This results in no limitation of available water to support the assumed higher potential evaporation transferring into actual evaporation. All these factors led to a transformation of the conceptual model from the basic one into the wetland model W.

3.3.4 Models P, E and M: XitaoXi Three models with differences in spatial distribution of climatic input data are test for the XitaoXi catchment in order to compare the results. They are: model P—lumped precipitation distribution and two sub-basin distributed ET_p; model E—lumped ET_p distribution and eight sub-basin distributed precipitation; and model M—spatial distribution in both precipitation and ET_p.

3.3.5 Model R: XitaoXi In the southeast upstream area of the XitaoXi catchment are the two reservoirs Fushishuiku and Laoshikan (near hydrostations 3 and 4 in Fig. 1). They are primarily used for irrigation during the dry season and flood

control during the rainy season. According to Jin and Gao (2006), the outflow from the reservoirs is controlled with some set-up water storage levels, as equation (13) suggests:

$$R_t = R_{t\text{-}1} + P_{rt} - Q_{rt} \tag{12}$$

$$Q_r = \begin{cases} 0\ (R \le Q_{\text{strict}}) \\ x\ (Q_{\text{strict}} < R < Q_{\text{normal}}) \\ y\ (Q_{\text{normal}} < R < Q_{\text{max}}) \\ z\ (R \ge Q_{\text{max}}) \end{cases} \tag{13}$$

where R_t is reservoir storage at time t; P_r is the net rainfall in the reservoir area; Q_r is the daily outflow from the reservoir; Q_{strict}, Q_{normal} and Q_{max} denote conservative storage, normal storage, flood storage, and x, y and z are defined outflow amounts from reservoir in different cases.

Both equations (12) and (13) describe the function of reservoir in our model R. Due to data restriction, it may be arguable that the large reservoirs are considered as points in the simulation (van der Knijff and de Roo 2008).

A short description of the main distinguishing features of all sub-modules is given in Table 1.

3.4 Parameter calibration

This study was made to investigate model structure as one of the sources of uncertainty, but it was quite difficult to calculate explicitly (Radwan *et al*. 2004, Lindenschmidt *et al*. 2007). However, each simple or combined model here has a different set of parameters, which needs to be calibrated; hence a strict division of parameter and structural uncertainty was not quantified. An automatic parameter calibration scheme (Schmitz *et al*. 2009) was employed in the PCRaster language environment to optimize parameter estimations for each model. This is designed as searching for the optimal parametric values targeting a high Nash-Sutcliffe value (Nash and Sutcliffe 1970). Given that the calibration result may lead to significant parameter uncertainty and equifinality between parameter sets, ten parameters sets coming from the simulation runs are retained for each model in terms of model capability to reproduce measured data. Therefore the model is consistent and can be meaningful for further model structure analysis. In this case, attention is given to the uncertainty in the process description represented by the model or sub-module ensembles and less to the uncertainty in the parameters.

3.5 Criteria for uncertainty evaluation

Traditionally, model performance is evaluated with different numeric criteria (Gupta and Sorooshian 1998, Krause *et al*. 2005). For this study we used Nash-Sutcliffe index (NS; Nash and Sutcliffe, 1970), regression coefficient R^2 and the difference of sum predicted and observed discharge values per year. These represent modelling efficiency, the match to the shape of the hydrographs and the water balance error, respectively. The combination of these three criteria is also used to decide which sub-modules will be included to form the cross-models.

We use two measures to quantify the deduced model prediction uncertainty. A normalized measure

Table 1 Short description of all sub-modules.

Basin	ID	Module description
Kielstau	H	ET_0 calculated with Haude method (DVWK 1996)
	M	ET_0 calculated with Penman-Monteith method
	L	Subsurface water flow from soil layer to river runoff
	T	Spatial distributed ET adjusted with land-use coefficients referring to Penman Monteith method (Allen *et al*. 1998)
	G	Outflow threshold of groundwater flow to river discharge
	D	Sub-surface drainage
	W	Additional wetland fraction (12%) in the soil zone, which has unlimited water support for evaporation as its actual ET equals the potential ET
XitaoXi	P	Lumped precipitation distribution and sub-basin distributed evapotranspiration
	E	Lumped evapotranspiration distribution and sub-basin distributed precipitation
	M	Sub-basin distributed precipitation and evapotranspiration
	G	Outflow threshold of groundwater flow to river discharge
	L	Subsurface water flow from soil layer to river runoff
	T	Spatial distributed evapotranspiration adjusted with land-use coefficients referring to Gao *et al*. (2006)
	R	Integration of two reservoirs in the upstream area referring to Jin and Gao (2006)

of the dispersion in the simulation ensemble was selected to indicate the influence of the variances in model structures on the uncertainty in flow simulations. This measure, termed *R* factor (Schuol and Abbaspour 2006), was defined as the average thickness of the prediction uncertainty among all ensemble runoff values at each time step normalized by the standard deviation of the measure data within a selected period. Another measure quantifying the strength of the model uncertainty is the *P* factor (Abbaspour *et al*. 2004), which is the percentage of measured data bracketed by the band of prediction uncertainty.

The ideal situation would be to have an *R* factor value close to zero, and in the meantime to bracket most of the measured data within the uncertainty band. This method is suitable for comparing ensemble dispersion of different scenarios and it is independent of the shape of the observed flows. The different contribution of the simulation uncertainty in low-flow and peak-flow seasons to the overall structural uncertainty will be assessed by examining patterns of behaviour in the *R* factor measure.

4 RESULTS AND DISCUSSION

4.1 Performance of model structure ensemble

According to the three criteria, the performances of all model structures of the two study basins are compared, as shown in Fig. 5. There are 17 models tested for each watershed, including seven simple and ten cross-models.

For the Kielstau basin, two simple models—H and T—did not perform as well as the basic module in any of the three criteria. Both models failed because of the evapotranspiration estimation. As expected, the Penman-Monteith method used in the basic model M can achieve a better result than the simple empirical Haude approach to calculate the potential evaporation. This may suggest that the Haude formula, especially the embraced monthly coefficients, needs further verification for a specific region before it can be applied in a model. This study shows that the summer evaporation is greatly underestimated and the growth of the plants starts earlier than predicted by the Haude method. The model T with an integration of land-use adjusted ET_0 has similar problems. The land-use coefficients referring to Penman-Monteith method did not help much to make a good estimation of the high evaporation rate at summer seasons. Models L and G could induce only little changes in model performance, with a minor improvement in the water balance error as the model G restrains groundwater recharging. Comparing the performance of all simple models shows that the influence of drainage and wetland fraction makes a great difference in model efficiency. The drainage process used in model D gives the most significant improvement. This can be observed in the performances of cross-models as well: models including drainage achieve relatively higher NS value and less water balance error. The combination of drainage and wetland fractions—model DW—outperformed hydrological simulations from all cross-models. Note that the Kielstau region is a very

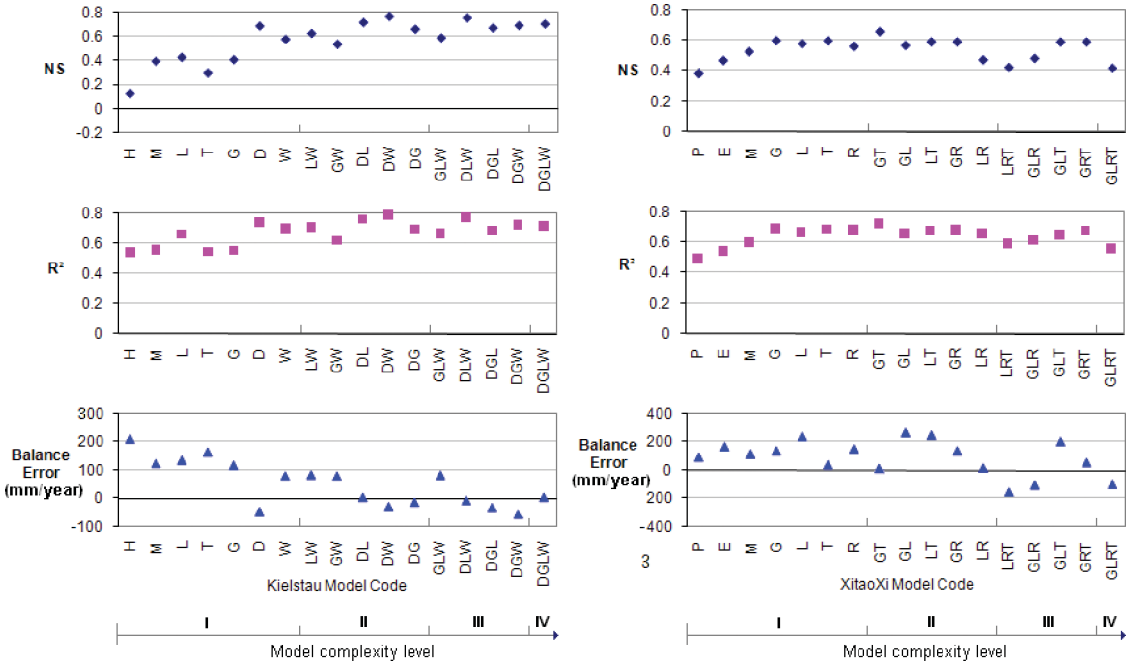

Fig. 5 Results of model efficiency NS, R^2 and summed water balance for all model structures.

flat landscape with open drainage ditches and a large area covered by wetlands; these must be essential elements in the local hydrological cycle. Moreover, the analysis of the Kielstau data set shows a low runoff to precipitation ratio with an average value of 0.318, whereas for Schleswig-Holstein, runoff is typically slightly below 50% of precipitation (Schmidtke 1999). Possible explanations for the lower discharge in summer and autumn (see Fig. 3) could be either that there is additional water loss by drainage and extra evapotranspiration is underestimated, or that the hydrological functions of e.g. wetland are ignored, or a part of both. Further data requirements and analysis are needed in support of the justification of these assumptions. The method of modelling with simple structure assumption here may provide useful information on the modelling uniqueness in this study area for any subsequent model applications. The well performing DW model shows that the integration of drainage and wetland fraction in the model creates a better fit of the simulated and measured runoff for the Kielstau basin. It decreases the large amount of excess runoff during the low flow periods. Water is extracted by the additional wetland storage mostly, drainage and high evaporation during summer and autumn seasons. It could thus represent the observed low runoff/precipitation characteristics in a better way. This may be the most appropriate model structure in all tested models for the catchment.

For the XitaoXi basin, the results of simple models demonstrate a strong link between the model performance and the spatial distribution of input climatic data. The model M with sub-basin distributed evaporation and precipitation has better performance than the model P and E in all three criteria. It is clear from the results that the regionalization of all hydroclimatological inputs should be handled with extreme care for large and mountainous watersheds like the XitaoXi basin. Therefore P and E were excluded from the cross-model procedure. Just two ET observation stations in model M can not provide sufficient information to quantify the spatial distribution of ET in the basin. Model T has shown further improvements in simulation results by updating ET data with land-use information. Furthermore, no significant enhancement in model simulation is observed in model L, the lateral flow model. This may suggest that the river discharge mainly comes from surface runoff since the dominant soil types are red soil and rocky soil, which tend to have limited water storage capacity and low permeability. A study from Xu *et al*. (2007) also indicates that saturation excess surface runoff is probably the dominant process for the XitaoXi catchment. The inclusion of two large reservoirs in the upstream basin (model R) did not improve the results drastically; it only decreased some peak discharges. The fact that large reservoirs are only modelled as points in the simulation may contribute to this, as significantly higher evaporation losses from the reservoir areas may be ignored. Among all the models, best performance is achieved by the model GT, which is coupled with groundwater outflow threshold, and spatial distribution of evaporation adjusted with land-use coefficients. It does not make a distinct increase in NS value, but a high R value and close-to-zero balance error may indicate that the runoff producing process of model GT suits the best to match the shape of hydrographs. This indicates to a certain extent that an appropriate input transformation process for the heterogeneous XitaoXi basin is a crucial step in model simulation, and the influence from the groundwater in the hilly region is very limited. The GT model structure may better capture the hydrological mechanisms reflected in the performance assessment.

Figure 5 also shows the complexity level of model structure indicated by the number of characters on its model ID. The model prediction ability is increasing to some extent with the model complexity level. At the first stage, the simple perceptual rainfall–runoff models perform relatively poorly for both watersheds. However, the most complicated model, which is coupled with all available sub-modules, does not necessarily report the best simulation result. Model performance depends strongly on model structure, but there is a trade-off between model complexity and simulation quality. The results demonstrate that the importance of various model structures is to a high degree case-dependent. The modules for the most significant improvement of model performance are different for two basins.

4.2 Model structural uncertainty analysis

An important goal for this paper is to highlight an example of structural uncertainty. Although it would be of some interest to break down the total uncertainty into its various components, it is quite difficult to do so and, as far as the authors are aware, no reliable procedure yet exists. It is generally impossible to exclude uncertainties from other sources owing to the inherent interrelations of all factors in any modelling procedure. For example, when the model structure is changed in any part of process description, it would unavoidably involve changes associated with system

input and calibration procedures. We can find a typical example of this, such as the sub-modules P, E and M in the XitaoXi models, which were more concerned with input data changes than with model structure. All the changes contribute to aggregate uncertainty so that it is difficult to tell the individual effect from each source. Therefore the uncertainty generated here account for all uncertainties.

However, this study endeavoured to focus on model structural analysis by investigating different perceptual models and to a large extent eliminating influences from other uncertainty sources. In this context, these prediction uncertainties are closely linked to the model structural errors arising from the aggregation of real world process into a modelling simplification.

The uncertainties are reflected in the discharge simulation presented in Fig. 6. The simulation results show a substantial variation in the hydrographs produced by the different model structures. This variation can be used as an estimate of the structure uncertainty of the selected models.

The shaded area in Fig. 6 represents the predicted simulation uncertainty for the years 1990–1995 in the Kielstau catchment, and for the years 1979–1983 in the XitaoXi basin. There is a high variation in model simulations caused by the different model structures. For the Kielstau catchment, 52.31% of the observed data (*P* factor) is bracketed by the uncertainty bound. The *R* factor is calculated as 0.58, which quantifies the thickness of the uncertainty bound. The predicted uncertainty band for the XitaoXi basin bracketed 61.54% of the observations, with an *R* factor of 0.51. It is notable that there are huge differences in runoff scales for the two basins in Fig. 6, which may explain why the dispersions of the ensemble model structures in the two basins are so different by visual comparison. The variation of all model simulations for the Kielstau catchment looks wider than that for the XitaoXi catchment. As these hydrographs for the Kielstau basin indicate, there is always a certain amount of diffusion and dispersion in the low flows, especially during summer seasons, and around the peaks. This gives rise to attenuation and modifications in the peak amplitude and shape, respectively, while the XitaoXi hydrographs give much tighter uncertainty bounds, and are generally centred on the observations. It has better results in the timing and magnitude of variations at any flow stages, with most of the peaks covered by the uncertainty band. However, the results for both basins are quantitatively similar. Judging from the two uncertainty measures, the derived perceptual model uncertainty bounds exhibit appropriate coverage (*P* factor $> 50\%$), and *R* factors are in the acceptable range (when it is small than 1, cf. Schuol and Abbaspour 2006). These reproduce the aggregation of all uncertainties, with explicit accounting for model structural errors. More accurate uncertainty bounds may be obtained by fitting distributions around the prediction of appropriate individual models, which would be a further parameter uncertainty research in future work.

4.3 Peak-flow low-flow split testing

To examine the uncertainty behaviour further, we use peak-flow low-flow split testing to take a closer look at the patterns of structural uncertainty. For comparison the monthly mean discharge data are plotted instead of the daily values. All months are divided

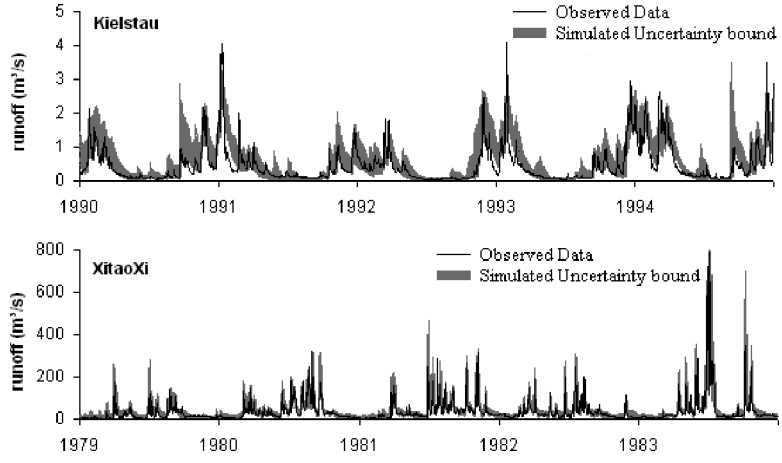

Fig. 6 Simulation results of different model structures for two study basins, with the shaded area showing the uncertainty intervals along with the measured discharge.

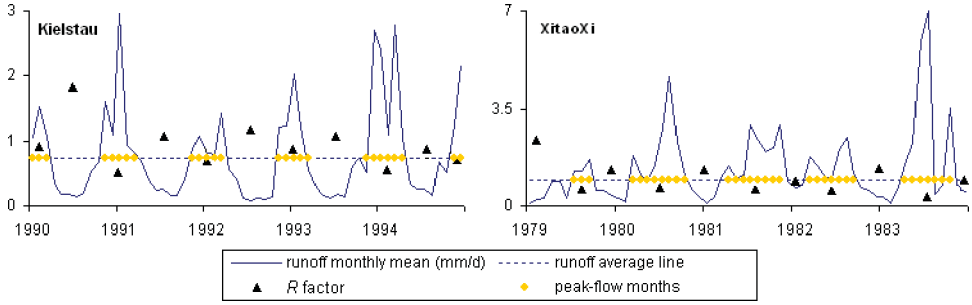

Fig. 7 Values of *R* factor for low-flow and peak-flow periods in the two study areas.

into peak-flow and low-flow seasons by the average discharge value of all years. Then the *R* factor is calculated for each season and the result is shown in Fig. 7. It reveals a clear pattern of how much each flow period contributed to the overall uncertainty during the whole period. Significantly smaller values are noted for the peak-flow months in Kielstau basin and higher values for low-flows. An analogous pattern is also observed for the completely different XitaoXi basin. Apparently low-flow seasons contribute more to the overall uncertainty than peak-flow seasons. It seems be more difficult to simulate river discharges at low-flow seasons. The results highlight problems related to the simulation of low flow. Worth mentioning is, that in a lot of papers about hydrological modelling (e.g. Yang *et al*. 2007) the authors argued that baseflow is easier to simulate, because in the peak-flow season, river flow may come from surface runoff, interflow and groundwater discharge, while in low-flow season, it is mainly dependant on groundwater discharge. It is obviously recognized that more factors have impacts on runoff generation during peak-flow time, but more uncertainty sources do not necessarily produce more prediction uncertainty in hydrological modelling. The power of influence from each factor on model simulation must be considered as well. Rainfall generally has the most significant impact on runoff generation, particularly in peak-flow season. And the relationship between rainfall and runoff is the most essential structure in all hydrological modelling. This rainfall–runoff relationship is thus better understood and implemented than other runoff-influencing factors such as groundwater and lateral flows. And in most cases rainfall is the major factor influencing runoff processes in peak-flow seasons. For those model structures with a dominating rainfall–runoff relationship, the peak-flows can be better reproduced. This is why we suggest that there are some other factors contributing to model uncertainty for low-flow seasons that need further investigation.

5 CONCLUSIONS

Modelling uncertainty associated with model structure errors is difficult to assess, not only theoretically, but also technically. This study developed a hydrological modelling framework that allows changes in model structure complexity, and investigated the structural uncertainty associated with river runoff simulations.

The simple KIDS hydrological model was tested for two watersheds with completely different characteristics. An extension of model structures with ensemble sub-modules was successfully applied to the implementation of the KIDS model. These models are plausible alternatives for the discharge simulation incorporating the main processes occurring in the selected river basins. We examined the impact of model structure on the hydrological simulations and evaluated the different model structures against a number of performance criteria for two study basins. Relating topological, geological and physical characteristics of the Kielstau River basin to the runoff simulation is essential for assessing the hydrological impacts of low gradient, wetland and high groundwater table in this basin. Since it is difficult to do such work with insufficient relevant data, some simplifying or assumptions are often necessary. Within the selected modelling framework, model DW performed better than other ones as it considered the possible influence of drainage and wetland. For the XitaoXi basin, accurate distributions of precipitation and evapotranspiration are two of the determining factors for the success of the river flow simulations. The two case studies indicated that hydrological models need careful site-specific priors and adaptations for a sound runoff simulation. It can also be concluded from the results that the extended KIDS model ensemble is generally applicable as a model structure test method for hydrological simulations under significantly different watershed conditions.

The related model structural uncertainty is estimated through the dispersion range of flow simulation ensembles around the observed data. Our approach leads to an acceptable mechanical and statistical description of simulation uncertainty, as quantified by the two measures—*P* factor and *R* factor. A peak-flow/low-flow split testing shows a similar pattern in both catchments: the uncertainties in baseflow are higher than in peak-flow periods. The reason for this is that, during the peak-flow or wet periods, the influence of other factors such as soil moisture or groundwater discharge is marginal, because of the dominant influence of rainfall, which is the factor that best accounted for runoff generation in our models.

Although some simplifications or assumptions in the model structure exploration might be arguable, we presented an effective method for practical model structural uncertainty estimations for the two study basins. Here, it was proved that an assumption and its model simplification (such as wetland in Kielstau or ET distribution in XitaoXi) are more critical than it may seem. In addition, all the adaptations in this paper have been based on field observations and data investigations, which greatly facilitated model analysis. Important conclusions that can be drawn from the results include: that wetlands must be a critical part of integrated water resources management in the Kielstau River basin, and that more refined climatological data would greatly increase model reliability for the XitaoXi catchment.

Finally, the variations in model simulations provided by the different model structures are interpreted as a result of the uncertainty in model structure. This incorporates a challenging problem of how to separate and define the model structural uncertainty explicitly. When only structural errors are inferred, the produced simulation uncertainties do not represent structural errors exclusively and are also contaminated by parameter estimation errors and input data errors. Hence, for this study, the simulation variations are considered to represent uncertainties mainly from structural errors but with influences from other uncertainty sources. Future work is recommended for further uncertainty investigation when considering other sources of uncertainty, such as parameter uncertainty and input data uncertainty. An attempt is made in this paper to strengthen the view that it is of great importance to explore different model structures to improve the overall accuracy of the simulations and to assess modelling uncertainty.

Acknowledgements We thank Kiel University, Germany, for financial support of this programme. We appreciate help from our colleagues of the Ecology Centre, Kiel University for access to their research data. We thank Nanjing Institute of Geography and Limnology, Chinese Academy of Sciences for the providing the XitaoXi data. Part of this work is sponsored by the National Research Programme (no. 2008CB418106) of the Chinese Ministry of Science and Technology; and by the Key Project (no. KZCX1-YW-14-6) of the Chinese Academy of Sciences. In addition, detailed reviews of two anonymous reviewers greatly improved the original manuscript.

REFERENCES

Abbaspour, K.C., Johnson, C.A. and van Genuchten, M.T., 2004. Estimating uncertain flow and transport parameters using a sequential uncertainty fitting procedure. *Vadose Zone J*., 3, 1340–1352.

Allen, R.G., Pereira, L.S., Raes, D. and Smith, M., 1998. Crop evapotranspiration—Guidelines for computing crop water requirements. Rome: Food and Agriculture Organization, *FAO Irrigation and Drainage Paper 56*. ISBN 92-5-104219–5.

Andersen, H.E., 2003. *Hydrology, nutrient processes and vegetation in floodplain wetlands*. PhD Thesis. National Environmental Research Institute, Denmark.

Beven, K., 2001. *Rainfall–Runoff Modelling*: *The Primer*: Chichester: Wiley.

Beven, K. and Binley, A., 1992. The future of distributed models—model calibration and uncertainty prediction. *Hydrol. Processes*, 6 (3), 279–298.

Beven, K. and Freer, J., 2001. Equifinality, data assimilation and uncertainty estimation in mechanistic modelling of complex environmental systems using the GLUE methodology. *J. Hydrol*., 249 (1–4), 11–29.

Beven, K., Smith, P. and Freer, J., 2007. Comment on "Hydrological forecasting uncertainty assessment: Incoherence of the GLUE methodology" by P. Mantovan and E. Todini. *J. Hydrol*., 338, 315–318.

Brown, J.D. and Heuvelink, G.B., 2005. Assessing uncertainty propagation through physically based models of soil water flow and solute transport. In: M. Anderson, ed. *Encyclopedia of Hydrological Sciences*. Chichester: Wiley, 1181–1196.

Bullock, A. and Acreman, M., 2003. The role of wetlands in the hydrological cycle. *Hydrol*. *Earth System Sci*., 7 (2), 358–389.

Butts, M.B., Payne, J.T., Kristensen, M. and Madsen, H., 2004. An evaluation of the impact of model structure on hydrological modelling uncertainty for streamflow simulation. *J. Hydrol*., 298, 242–266.

Carpenter, T.M. and Georgakakos, K.P., 2004. Impacts of parametric and radar rainfall uncertainty on the ensemble streamflow simulations of a distributed hydrologic model. *J. Hydrol.*, 298, 202–221.

Choi, H.T. and Beven, K.J., 2007. Multi-period and multi-criteria model conditioning to reduce prediction uncertainty in an application of TOPMODEL within the GLUE framework. *J. Hydrol*., 332, 316–336.

Christiaens, K. and Feyen, J., 2002. Constraining soil hydraulic parameter and output uncertainty of the distributed hydrological

MIKE SHE model using the GLUE framework. *Hydrol. Processes*, 16, 373–391.

Clausnitzer, V., Hopmans, J.W. and Starr, J.L., 1998. Parameter uncertainty analysis of common infiltration models. *Soil Sci. Soc. Am. J*., 62, 1477–1487.

DVWK (Deutscher Verband für Wasserwirtschaft und Kulturbau e.V.), 1996. Ermittlung der Verdunstung von Land- und Wasserflächen. Bonn: DVWK, Merkblätter zur Wasserwirtschaft, Heft 238 (1996), 135.

Ewen, J., O'Donnell, G., Burton, A. and O'Connell, E., 2006. Errors and uncertainty in physically-based rainfall–runoff modelling of catchment change effects. *J. Hydrol*., 330 (3–4), 641–650.

Gao, J., Lu, G., Zhao, G. and Li, J., 2006. Watershed data model: a case study of Xitiaoxi sub-waterhed, Taihu Basin (in Chinese, with English abstract). *J. Lake Sciences*, 18 (3), 312–331.

Glugla, G., 1969. Berechnungsverfahren zur Ermittlung des aktuellen Wassergehalts und Gravitationswasserabflusses im Boden. *Albrecht-Thaer-Archiv*, 13 (4), 371–376.

Gourley, J. and Vieux, B., 2006. A method for identifying sources of model uncertainty in rainfall–runoff simulations. *J. Hydrol*., 327, 68–80.

Gupta, H.V., Beven, K.J. and Wagener, T., 2005. Model calibration and uncertainty estimation. In: M. Anderson, ed. *Encyclopedia of Hydrologic Sciences*. Chichester: Wiley.

Gupta, H.V. and Sorooshian, S., 1998. Toward improved calibration of hydrologic models: multiple and noncommensurable measures of information. *Water Resour*. *Res*. 34 (4), 751–763.

Haan, C.T., Storm, D.E., Al-Issa, T., Prabhu, S., Sabbagh, G.J. and Edwards, D.R., 1998. Effect of parameter distributions on uncertainty analysis of hydrologic models. *Trans. Am. Soc. Agric. Engrs*, 41, 65–70.

Hansen, S., Thorsen, M., Pebesma, E.J., Kleeschulte, S. and Svendsen, H., 1999. Uncertainty in simulated nitrate leaching due to uncertainty in input data. A case study. *Soil Use Manag*., 15, 167–175.

Haude, 1958. Ueber die Verwendung verschiedener Klimafaktoren zur Berechnung der Evaporation und Evapotranspiration. *Meteorol. Rundschau*, 11, 96–99.

Hörmann, G., Zhang, X. and Fohrer, N., 2007. Comparison of a simple and a spatially distributed hydrologic model for the simulation of a lowland catchment in Northern Germany. *Ecol. Modelling*, 209 (1), 21–28.

Jin, X. and Gao, J., 2006. *Modelling of human activities impacts to hydrological processes—based on distributed hydrological model* (in Chinese, with English abstract). MSc Thesis, Nanjing Institute of Geography & Limnology, Chinese Academy of Sciences.

Krause, P., Boyle, D.P. and Baese, F., 2005. Comparison of different efficiency criteria for hydrological model assessment. *Adv. Geosci*., 5, 89–97.

Lindenschmidt, K.E., 2006. The effect of complexity on parameter sensitivity and model uncertainty in river water quality modelling. *Ecol. Modelling*, 190, 72–86.

Lindenschmidt, K.E., Fleischbein, K. and Baborowski, M., 2007. Structural uncertainty in a river water quality modelling system. *Ecol. Modelling*, 204, 289–300.

Melching, C.S., 1995. Reliability estimation. In: V. Singh, ed. *Computer Models of Watershed Hydrology*. Littleton, CO: Water Resources Publications, 69–118.

Nash, J.E. and Sutcliffe, J.V., 1970. River flow forecasting through conceptual models. Part I: A discussion on principles. *J Hydrol*., 10, 282–290.

Neuman, S.P., 2002. Accounting for conceptual model uncertainty via maximum likelihood Bayesian model averaging. *Acta Univ. Carolinae Geologica*, 46 (2/3), 529–534.

Radwan, M., Willems, P. and Berlamont, J., 2004. Sensitivity and uncertainty analysis for river quality modelling. *J. Hydroinform*. 6, 83–99.

Ratto, M., Young, P.C., Romanowicz, R., Pappenberger, F., Saltelli, A. and Pagano, A., 2007. Uncertainty, sensitivity analysis and the role of data based mechanistic modelling in hydrology. *Hydrol. Earth System Sci*., 11, 1249–1266.

Rogers, C.C.M., Beven, K.J., Morris, E.M. and Anderson, M.G., 1985. Sensitivity analysis, calibration and predictive uncertainty of the institute of hydrology distributed model. *J. Hydrol*., 81, 179–191.

Schmidtke, K.D., 1999. *Land im Wind—Wetter und Klima in Schleswig-Holstein*. Wachholtz Verlag.

Schmitz, O., Karssenberg, D., van Deursen, W.P.A. and Wesseling, C.G., 2009, Linking external components to a spatio-temporal modelling framework: coupling MODFLOW and PCRaster. *Environ. Model. Software*, 24, 1088–1099.

Schuol, J. and Abbaspour, K. C., 2006. Calibration and uncertainty issues of a hydrological model (SWAT) applied to West Africa. *Adv. Geosci*., 9, 137–143.

Son, K. and Sivapalan, M., 2007. Improving model structure and reducing parameter uncertainty in conceptual water balance models through the use of auxiliary data. *Water Resour. Res*., 43 (1), doi:10.1029/2006WR005032.

Sponagel, H., 2005. *Bodenkundliche Kartieranleitung*. Hannover: Adhocarbeitsgruppe Boden der Staatlichen Geologischen Dienste und der Bundesanstalt für Geowissenschaften und Rohstoffe. 5. Verbesserte und erweiterte Auflage.

Springer, P., 2006. *Analyse der Interaktion zwischen Oberflächenwasser und Grundwasser am Beispiel einer Flussniederung im Norddeutschen Tiefland*. Diplomarbeit, Fach Geographie, Christian-Albrechts-Universität zu Kiel, Germany.

Takagi, K., Tsuboya, T. and Takahashi, H., 1998. Diurnal hystereses of stomatal and bulk surface conductances in relation to vapor pressure deficit in a cool temperate wetland. *Agric. For. Met*., 91, 177–191.

Trepel, M., 2004. Development and application of a GIS-based peatland inventory for Schleswig Holstein (Germany). In: J. Päivänen, ed. *Proceedings of the 12th International Peat Congress—Wise Use of Peatlands*, vol. 2, 931–936.

Uhlenbrook, S., Seibert, J., Leibundgut, Ch. and Rodhe, A., 1999. Prediction uncertainty of conceptual rainfall–runoff models caused by problems to identify model parameters and structure. *Hydrol. Sci*. *J*., 44 (5), 279–299.

Van der Knijff, J. and de Roo, A., 2008. *LISFLOOD Distributed Water Balance and Flood Simulation Model*, Revised user manual. Luxembourg: Office for Official Publications of the European Communities, EUR 22166 EN/2.

Van Deursen, W.P.A., 1995. *Geographical Information Systems and Dynamic Models: development and application of a prototype spatial modelling language*. Netherlands Geographic Studies, Issue 190.

Vrugt, J.A., Clark, M.P. and Diks, C.G.H., 2006. Multi-objective calibration of forecast ensembles using Bayesian model averaging. *Geophys. Res*. *Lett*., 33 (19), 1–6.

Vrugt, J.A., Diks, C.G.H., Gupta, H.V., Bouten, W. and Verstraten, J.M., 2005. Improved treatment of uncertainty in hydrologic modelling: combining the strengths of global optimization and data assimilation. *Water Resour. Res*., 41 (1), 1–17.

Wan, R., Yang, G., Li, H. and Yang L., 2007. Simulating flood events in a mesoscale watershed: a case study from River Xitiaoxi Watershed in the upper region of Taihu basin. *J. Lake Sci*., 19 (2), 170–176.

Wesseling, C.G., Karssenberg, D.J., Burrough, P.A. and Van Deursen, W.P.A., 1996. Integrated dynamic environmental models in GIS: the development of a dynamic modelling language. *Trans. GIS*, 1 (1), 40–48.

Wu, K. and Johnston, C.A., 2008. Hydrologic comparison between a forested and a wetland/lake dominated watershed using SWAT. *Hydrol. Processes*, 22, 1431–1442.

Xu, L., Zhang, Q., Li, H., Viney, N.R., Xu, J. and Liu, J., 2007. Modelling of surface runoff in Xitiaoxi catchment. China. *Water Resour. Manage*., 21, 1313–1323, doi:10.1007/s11269-006-9083–6.

Yang, J., Reichert, P. and Abbaspour, K.C., 2007. Bayesian uncertainty analysis in distributed hydrologic modelling: a case study in the Thur River basin (Switzerland). *Water Resour. Res*., 43, W10401, doi:10.1029/2006WR005497, 1–13.

Zhang, Q., Li, H. and Xu, L., 2006. Surface runof modelling for Xitiaoxi catchment, Taihu Basin. *J. Lake Sci*., 18 (4), 401–406.

Zhang, X., Hörmann, G. and Fohrer, N., 2007. The effects of different model complexity on the quality of discharge simulation for a lowland catchment in northern Germany. Heft 20.07 *Einfluss von Bewirtschaftung und Klima auf Wasser- und Stoffhaushalt von Gewässern* (2007), Band 2, Forum für Hydrologie und Wasserbewirtschaftung, ISBN 978-3-940173-04-1.

Zhang, X., Hörmann, G. and Fohrer, N., 2008. An investigation of the effects of model structure on model performance to reduce discharge simulation uncertainty in two catchments. *Adv. Geosci*., 18, 31–35.

Zhang, X., Hörmann, G. and Fohrer, N., 2009. Hydrologic comparison between a lowland catchment (Kielstau, Germany) and a mountainous catchment (XitaoXi, China) using KIDS model in PCRaster. *Adv. Geosci*., 7, 1–6.